A Repainting Algorithm for a Color Image Using Pixel Modulation Based on the Statistic Properties of Image's Pixels

Chen-Chung Liu
Department of Electronic Engineering
National Chin-Yi University of Technology
ccl@ncut.edu.tw

Guan-Nan Hu
Department of Electronic Engineering
National Chin-Yi University of Technology
Robert6pill@gmail.com

Abstract—This paper presents a simple and powerful algorithm to automatically repaint a color image. This new approach uses the pixel transformation based on the correlation between the distribution of the original image and the distribution of the reference image. The presented scheme first finds the original image pixels' distribution and the reference image pixels' distribution in R plane, G plane, and B plane, respectively. Each plane then is transformed into Gaussian distribution, respectively and simultaneously. In each plane, the presented scheme uses the linear regression to find the best fitting function for the transformed data of original image and the transformed data of reference image. The repainting transformed data is calculated by the best fitting function. Finally, the repainting data is obtained by taking the inverse transformation of the repainting transformed data.To explore the utility and demonstrate the efficiency of the proposed algorithm, simulations under various input images were conducted. The experiment results showed that our proposed algorithm can precisely simulate the desired scenes at an assigned time and has two advantages: (a) Using the best fitting function to determine the pixel value of each pixel to repaint the color image is time saving largely. (b) It is also time saving by directly taking the repainting on RGB domain instead of other domains, because it does not need any domain transformation.

Keywords—repaint, Gaussian distribution, linear regression, transformation, best fitting function.

1. INTRODUCTION

Reflected light from an object is the product of surface spectral reflectance and illumination spectral power distribution. Consequently, illumination color significantly determines the object's color appearance. The object color appearance changes accordingly when the illumination color changes. This leads to many problems in algorithms of computer vision. For example, the illumination change in creating a realistic model causes the color appearance of an object to be inconsistent [1].

Color is one important source of information for out- door image analysis, classification, segmentation, recognition, and retrieval[2]. Unfortunately, out-door scene images obtained from capturing devices, are severely influenced by the spectral and spatial distribution of lighting in the scene. And, outdoor scenes are particularly hard to treat in terms of lighting conditions due to weather phenomena, time of day and seasons. [3]

Earth's atmosphere contains both air molecules and tiny aerosols (much tinier than the wavelength of the visible light from Sun) - both of them scatter the visible light from the Sun which grazes Earth's atmosphere. The scattering from both air molecules and aerosols is predominantly the Rayleigh scattering [4- 7]. According to the Rayleigh scattering law of light, blue light is scattered more than the red light. When the sun is relatively vertical to the horizon, its light goes through very little atmosphere, so little scattering takes place, hence the sky far away from the sun appears light blue at noon. Conversely, approaching to sunrise or sunset, Sunlight has to travel through a much thicker layer of atmosphere to reach us on the ground. This extra distance causes multiple scatterings of blue light, the sky appears less bright and redder than that at noon because more blue light than red light is scattered out of the solar light-rays, leaving an excess of red light.

It is very difficult to obtain the concentration and the diameters of the air molecules and the tiny aerosols in the Earth's atmosphere so it is impossible to estimate the colors of an outdoor scene precisely by using the Rayleigh scattering law of light. In 2002, Thompson derived a spatial post- processing algorithm of night scene [8] based on the visual noise (VN) and the loss of acuity (LA).It can generate more realistic night scene, but it cannot clearly illustrate the differences between different times during the entire night because of its neglecting for the time factor. Alexander Toet used the method introduced by Welsh et al to transfer a source image's color characteristics to a grayscale target image (night vision imagery)[9,10]. They transformed both the source image and the target image that resembles the target scenes into a perceptually miscorrelated color space. In the miscorrelated color space, they searched the best matching source pixel from the source image for each target pixel by using the first order statistics of the luminance distribution in a 7×7 window around the source and target pixels. Finally, they assigned the matching pixel's chromaticity values of the source image to the target pixel. Although they effectively give single-band intensified night vision gray imagery a full color day-time image, but to find a suitable resembled color source image for the target image is not easy, and the final colors of the chromatic target image completely depends on the colors of the source image. They are not the true colors of the target image taken in day. Other papers about the scenes can be found in [11-15]

The Gaussian distribution is first derived by De Moivre and later by both Gauss and Laplace. The Gaussian distribution is the most widely useful distribution; it frequently appears in nearly all areas of science, engineering, commerce, and so on. These important properties of its precise description of many practical and significant real world quantities are the result of many small independent random effects acting to generate the quantity of interest. The presented algorithm uses the pixel transformation based on the correlation between the distribution of the original image and the distribution of the reference image. The presented scheme first finds the original image pixels' distribution and the reference image pixels' distribution in R plane, G plane, and B plane, respectively. Each plane then is transformed into Gaussian distribution, respectively and simultaneously. In each plane, the presented scheme uses the linear regression to find the best fitting function for the transformed data of original image and the transformed data of reference image. The repainting transformed data is calculated by the best fitting function. Finally, the repainting data is obtained by taking the inverse transformation of the repainting transformed data. The red, green and blue are the primary components of light (or color image) in spatial domain. The spatial pixels of an image are often correlative, so the spatial domain of an image is very suitable for taking repainting.

. The remainder of this paper is organized as follows: Section 2 presents the repainting algorithm of color image. Empirical results are described in the Section 3. Finally, Section 4 concludes this paper.

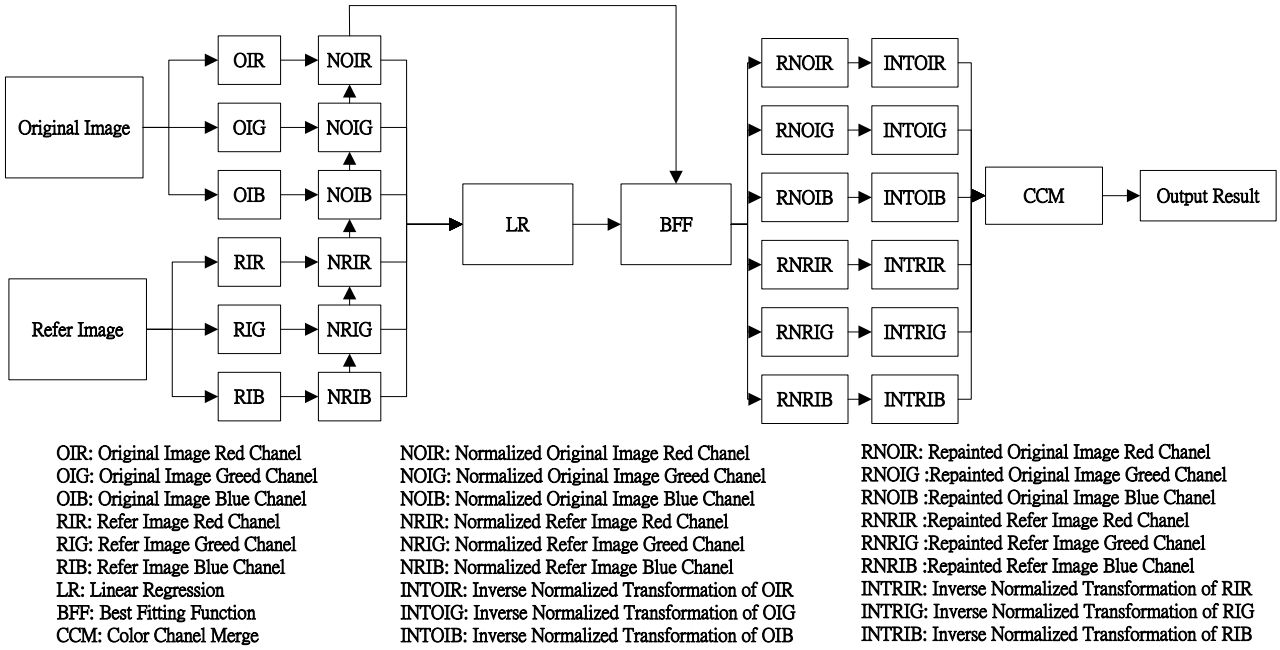

Fig. 1 The flow chart of the presented algorithm of color image repainting

2. THE PRESENTED RE-COLORIZING ALGORITHM

The presented scheme first finds the original image pixels' distribution and the reference image pixels' distribution in L* plane, a* plane, and b* plane, respectively. Each plane then is transformed into Gaussian distribution, respectively. In each transferred plane, the presented scheme uses the multiple regression to find the best fitting functions for the transformed data of original image. The re-colorizing transformed data is calculated by the best fitting functions. Finally, the re-colorizing data is obtained by taking the inverse transformation of the re- colorizing transformed data. Fig. 1 shows the flow chart of the presented re- coloring algorithm. The more detail description of the presented algorithm is illustrated in the follow

2.1 The RGB color system

The color of an object can be explained scientifically as the color of light reflected by the particular object (while lights of other colors being absorbed). Although the range of colors is infinite, the range of colors which is perceivable by human visual system can be produced by the mixtures of finite visual lights of various wavelengths. Human eyes have three different cone shaped light receptors [16-18]. Each cone receptor is sensitive to a special range of colors. One is sensitive to primarily red, another to primarily green, and another to primarily blue. Each cone receptor transmits a neural pulse to the brain at a rate proportional to the light's intensity. By combining the signal rates transmitted from three cone receptors, the brain is able to interpret color and brightness of the light perceived. Hence, by combining different proportions of the three colors (red, green and blue), a full range of perceivable colors by human eyes is able to be reproduced.

In televisions, computer monitors, and colored image projection systems, by using only the three colors are enough to adequately represent any of the unlimited visible colors [19,20]. For measuring or reproducing color, a number of three dimensional color models have been defined; Color models like as HIS, L*a*b*, YIQ, YUV, and YCbCr are suitable for

image processing applications, they are obtained by some color transform from RGB color space, They are suitable for image processing applications, but not suitable for the color representation of a color image. The image in RGB color space is not suitable for image processing applications because the image in RGB color space is highly correlated, but it is the most suitable for the color representation of a color image. The RGB color model is the most popular and natural color model, due to it can compose any color adequately. R, G and B component of a color in RGB color space are given by:

$$R,G,B = k\int_{400}^{700} I(\lambda)\Phi(\lambda)S_{R,G,B}(\lambda)d\lambda \quad (1)$$

where k is a constant that defines the total overall brightness response of the human eyes, $I[\lambda]$ is the illumination spectral intensity of a color, $\Phi[\lambda]$ is the object spectral reflectivity, $S_{R,G,B}[\lambda]$ is the spectral sensitivity of the R or G or B channel of the detector and λ is the wavelength. The normalized red, green, and blue coordinates are defined as follow:

$$r = R/(R+G+B) \quad (2)$$

$$g = G/(R+G+B) \quad (3)$$

$$b = B/(R+G+B) \quad (4)$$

where R, G and B are the intensities of red, green, and blue light at a given pixel [21.22]. In order to obtain the more accuracy regression of a scene image, we spilt the original image into its R, G, and B components firstly.

2.2 Gaussian Distribution

The Gaussian distribution is first derived by De Moivre and later by both Gauss and Laplace. The Gaussian distribution is the most widely useful distribution; it frequently appears in nearly all areas of science, engineering, commerce, and so on. This important properties of its precise description of many practical and significant real world quantities, especially when such quantities are the result of many small independent random effects acting to generate the quantity of interest. The Gaussian density function is described by the probability density function

$$f(x) = \frac{1}{\sqrt{2\pi\sigma^2}} e^{-(x-\mu)^2/2\sigma^2} \quad (5)$$

which is symmetric about x .The maximum value is $1/\sqrt{2\pi\sigma^2}$ appears at $x = \mu$. Its spread about the point $x = \mu$ is related to σ. The function value decreases to 0.607 times its maximum at $x=\mu+\sigma$ and $x=\mu-\sigma$. For the Gaussian distribution, then 68% of events fall within 1σ,95% of events fall within 2σ,97.7% of events fall within 3σ.

2.3 The Linear regression

When performing experiment, we frequently tabulate data in the form of ordered pairs $(x_1,y_1),(x_2,y_2),...,(x_n,y_n)$ with each x_i distinct. Given the data, it is then usually desirable to be able to predict y from x by finding a mathematical model, that is, a function $y = H(x)$ that fits the data as closely as possible. One way to determine how well the function $y = H(x)$ fits these order pairs $(x_1,y_1),(x_2,y_2),...,(x_n,y_n)$ is to measure the sum of squares of the errors (SSE) between the predicted values of y and the observed values y_i for all of the n data points.

Linear regression is one of the widely used statistical techniques [43, 44]. This technique is used to find a polynomial function of degree k, $y = \beta_0 + \beta_1 x + \beta_2 x^2 + ... + \beta_k x^k$ as the predicting function, that has the minimum of the sum of squares of the errors(SSE) between the predicted values of y and the observed values y_i for all of the n data points $(x_1,y_1),(x_2,y_2),...,(x_n,y_n)$.The values of β_0, β_1, β_2 ,…, and β_k that minimize

$$SSE(\beta_0,\beta_1,\ldots,\beta_k) = \sum_{i=1}^{n}\left[Y_i - (\beta_0 + \beta_0\beta x_i + \beta_2 x_i^2 + \cdots + \beta_k x_i^k)\right]^2 \quad (6)$$

are obtained by setting the $k+1$ first partial derivatives $\frac{\partial}{\partial\beta_0} SSE(\beta_0,\beta_1,...,\beta_k)$,

$\frac{\partial}{\partial \beta_1} SSE(\beta_0, \beta_1, ..., \beta_k)$, …, and $\frac{\partial}{\partial \beta_k} SSE(\beta_0, \beta_1, ...\beta_k)$ equal to zero, and solving the resulting simultaneous linear system of the so-called normal equations:

$$n\beta_0 + \beta_1 \sum_{i=1}^{n} x_i + \beta_2 \sum_{i=1}^{n} x_i^2 + \cdots + \beta_k \sum_{i=1}^{n} x_i^k = \sum_{i=1}^{n} Y_i \quad (7)$$

$$\beta_0 \sum_{i=1}^{n} x_i + \beta_1 \sum_{i=1}^{n} x_i^2 + \cdots + \beta_k \sum_{i=1}^{n} x_i^k = \sum_{i=1}^{n} x_i Y_i \quad (8)$$

$$\beta_0 \sum_{i=1}^{n} x_i^k + \beta_1 \sum_{i=1}^{n} x_i^{k+1} + \cdots + \beta_k \sum_{i=1}^{n} x_i^{2k} = \sum_{i=1}^{n} Y_i x_i^k \quad (9)$$

, and the matrix form solution of the normal equations system be

(a)Original Image

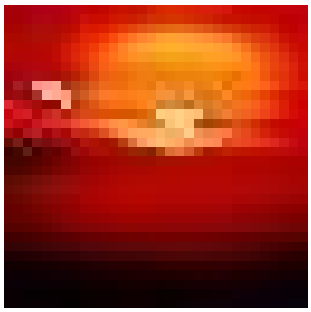

(b)Reference Image

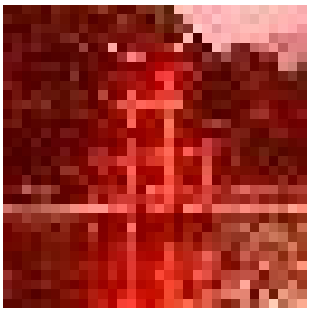

(c)Repainted Image

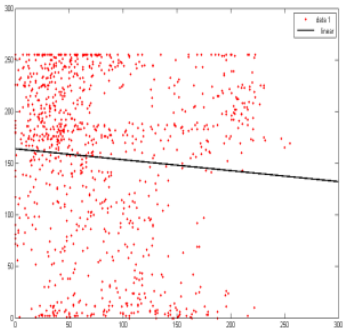

(d)R plane

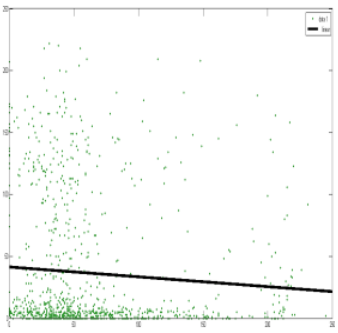

(e)G plane

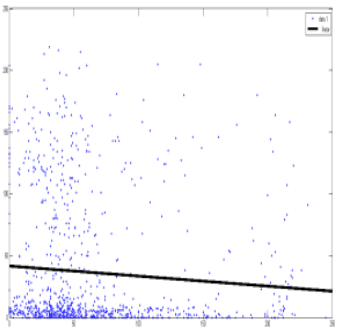

(f)B plane

Fig. 2. The linear regression of the original color image and the reference color image;(a)Original color image, (b)Reference color image, (c)Repainted color image, (d)the linear regression in the R plane, (e) the linear regression in the G plane, (f) the linear regression in the B plane.

(a) Original Image

(b) Reference Image

(c) Repainted Image

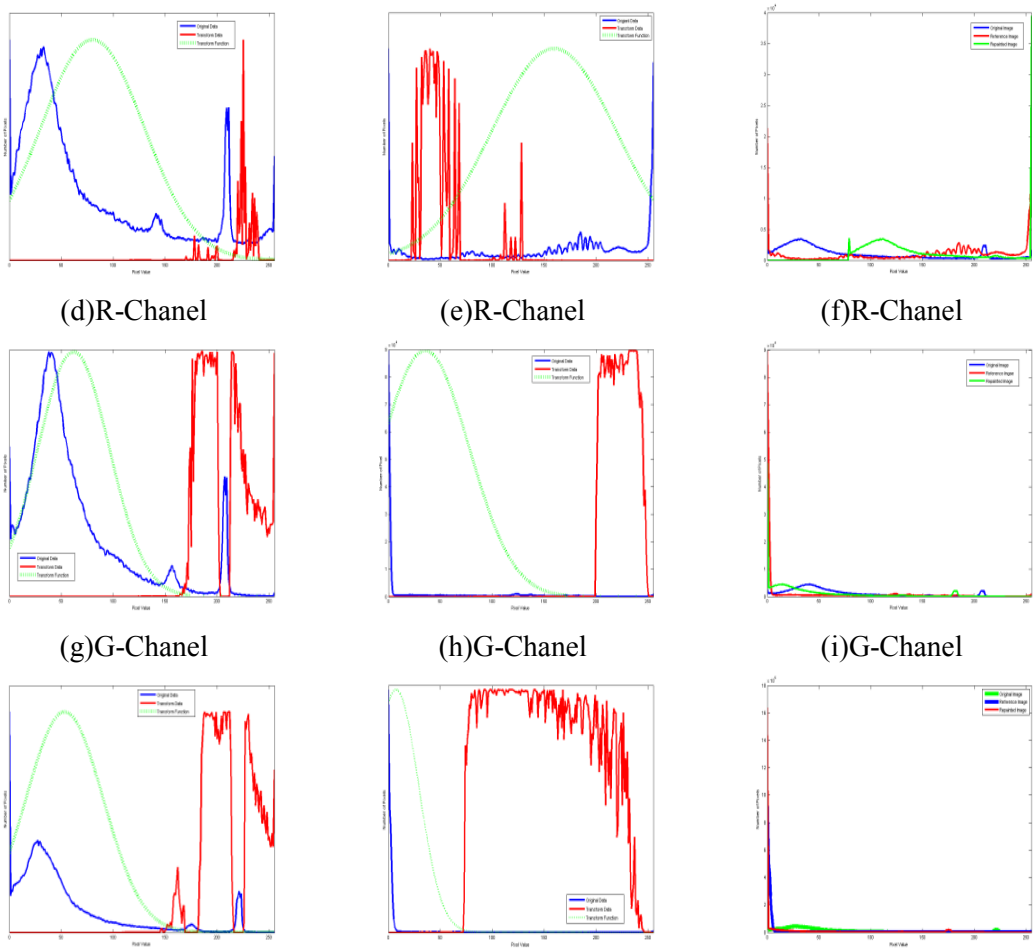

(d)R-Chanel (e)R-Chanel (f)R-Chanel

(g)G-Chanel (h)G-Chanel (i)G-Chanel

(j)B-Chanel (k)B-Chanel (l)B-Chanel

Fig. 3. simulation results, (a) Original Image, (b) Refer Image, (c)Repainted image, (d) R-Chanel of (a), (e) R-Chanel of (b), (f) R-Chanel of (c) , (g) G-Chanel of (a), (h) G-Chanel of (b), (i) G-Chanel of (c), (j) B-Chanel of (a), (k) B-Chanel of (b), (l) B-Chanel of (c).

TABLE 1: THE STATISTIC VALUES OF FIG.3.

	Original Image	**Reference Image**	**Repainted Image**
MR	79.9461	159.3727	152.8975
MG	61.7109	35.3308	37.7732
MB	53.0032	7.2787	20.9327
SR	70.0282	85.3229	58.2491
SG	48.5672	59.8086	46.6071
SB	52.6069	30.7386	44.2373

$$\begin{bmatrix} \beta_0 \\ \beta_1 \\ \beta_2 \\ \vdots \\ \beta_k \end{bmatrix} = \mathrm{B} = \left[X^T X\right]^{-1}\left[X^T Y\right]$$

(10)

,where

$$X = \begin{bmatrix} 1 & x_1 & x_1^2 & \dots & x_1^k \\ 1 & x_2 & x_2^2 & \dots & x_2^k \\ 1 & x_3 & x_3^2 & \dots & x_3^k \\ \vdots & \vdots & \vdots & \vdots\vdots & \vdots \\ 1 & x_n & x_n^2 & \dots & x_n^k \end{bmatrix},$$

$$Y = \begin{bmatrix} y_1 \\ y_2 \\ \vdots \\ y_n \end{bmatrix} \qquad (11)$$

Figure 2 shows the linear regression in the R plane, G plane, and the B plane of a 32*32

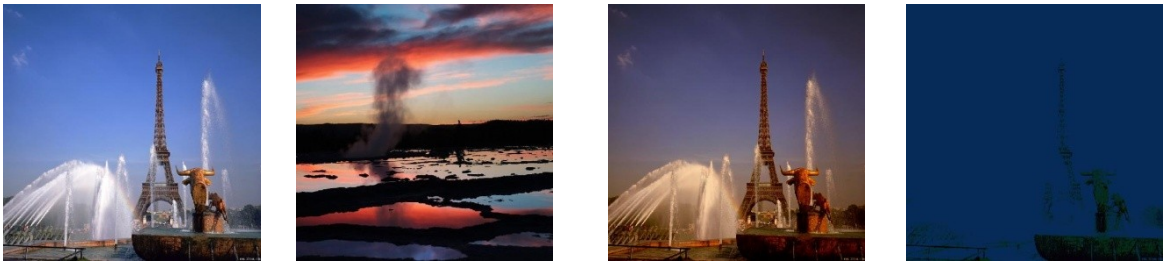

(a)Original Image (b) Reference Image (c)Repainted Image (d)Difference Image

Fig. 4. simulation images, (a)original image, (b) reference image, (c) repainted image, (d)the difference image between the original image and the repainted image.

TABLE 2: THE STATISTIC VALUES OF FIG.4.

	Original Image	**Reference Image**	**Repainted Image**
MR	101.899	95.6056	95.904
MG	118.2243	74.9931	76.7079
MB	164.7212	76.4277	82.6985
SR	46.7933	80.7548	46.7829
SG	42.8885	65.9013	39.5958
SB	56.8072	61.4968	43.53

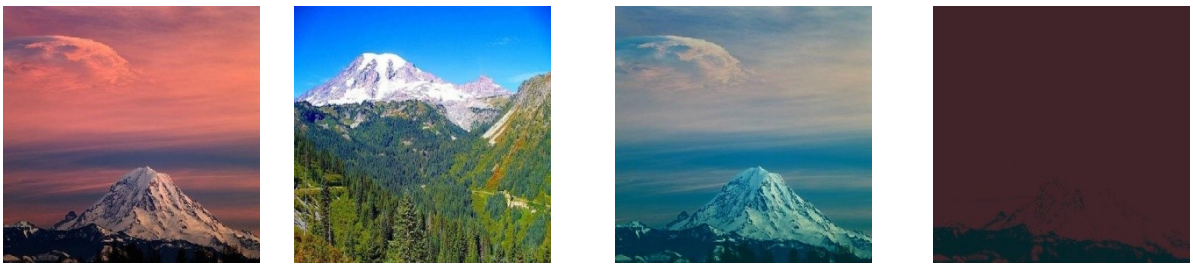

(a)Original Image (b) Reference Image (c) Repainted Image (d) Difference Image

Fig. 5. simulation images, (a)original image, (b) reference image, (c) repainted image, (d)the difference image between the original image and the repainted image.

TABLE 3: THE STATISTIC VALUES OF FIG.5

	Original Image	**Reference Image**	**Repainted Image**
MR	146.4322	81.8842	86.9693
MG	89.1814	125.0496	125.181
MB	93.7952	135.3151	135.7946
SR	68.7051	65.9391	59.0253
SG	33.7305	51.2038	33.7289
SB	28.3915	91.1322	28.3885

(a)Original Image (b) Reference Image (c) Repainted Image (d) Difference Image

Fig. 6. simulation images, (a)original image, (b) reference image, (c) repainted image, (d)the difference image between the original image and the repainted image.

TABLE 4: THE STATISTIC VALUES OF FIG.6

	Original Image	Reference Image	Repainted Image
MR	132.9273	101.6116	102.0284
MG	150.0663	76.5998	77.854
MB	169.3153	69.8364	72.9481
SR	54.9274	55.3663	54.7244
SG	48.5555	35.768	47.0828
SB	48.3282	31.1784	43.1924

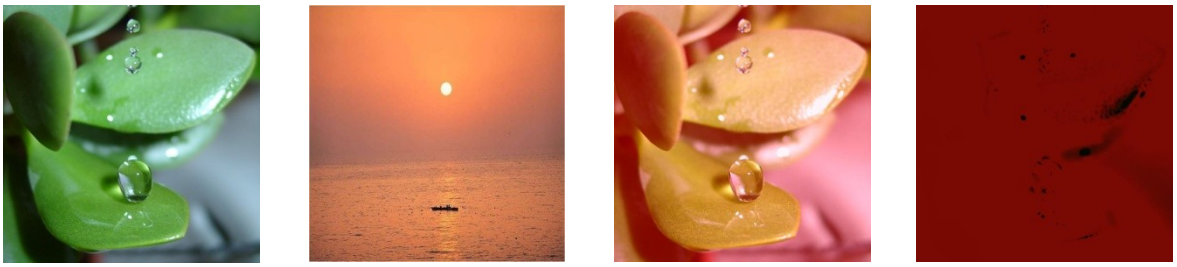

(a)Original Image (b) Reference Image (c) Repainted Image (d) Difference Image

Fig. 7. simulation images, (a)original image, (b) reference image, (c) repainted image, (d)the difference image between the original image and the repainted image.

TABLE 5: THE STATISTIC VALUES OF FIG.7

	Original Image	Reference Image	Repainted Image
MR	**90.043**	**210.531**	**207.554**
MG	**132.697**	**123.987**	**123.697**
MB	**88.731**	**85.422**	**85.861**
SR	**44.341**	**32.349**	**40.221**
SG	**57.234**	**20.843**	**57.234**
SB	**61.707**	**14.314**	**61.525**

original color image and a 32*32 reference color image.

Figure 4- Figure 7 and table 2- table 5 are also used to illustrate the performance of the presented algorithm. Fig. 4(a) is the original image taken in afternoon, Fig. 4(b) is the reference image taken at dusk, Fig. 4(c) is

the repainted image, and Fig. 4(d) is the absolute difference image between the original image and the repainted image. On the other hand, Table 2 shows the statistic characteristics (mean, standard deviation in R, G, B plane, respectively) of the three images (original, reference, and repainted) of figure 4.

Fig. 5(a) is the original image taken in afternoon, Fig. 5(b) is the reference image taken at dusk, Fig. 5(c) is the repainted image, and Fig. 5(d) is the absolute difference image between the original image and the repainted image. On the other hand, Table 3 shows the statistic characteristics (mean, standard deviation in R, G, B plane, respectively) of the three images (original, reference, and repainted) of figure 5.

Fig. 6(a) is the original image taken in afternoon, Fig. 6(b) is the reference image taken at dusk, Fig. 6(c) is the repainted image, and Fig. 6(d) is the absolute difference image between the original image and the repainted image. On the other hand, Table 4 shows the statistic characteristics (mean, standard deviation in R, G, B plane, respectively) of the three images (original, reference, and repainted) of figure 6.

Fig. 7(a) is the original image taken in afternoon, Fig. 7(b) is the reference image taken at dusk, Fig. 7(c) is the repainted image, and Fig. 7(d) is the absolute difference image between the original image and the repainted image. On the other hand, Table 5 shows the statistic characteristics (mean, standard deviation in R, G, B plane, respectively) of the three images (original, reference, and repainted) of figure 7.

Previous experiment results show that the presented algorithm treats RGB channels independently can give much sharper results. Another good feature of the presented algorithm is that the repainted are more realistic compared to other methods.

4.CONCLUSION

For color image re-colorizing simulation using a computer with Intel Pentium D 2.80GHz CPU and 512MB RAM, it only takes less than 0.8 second to re-colorize a color image of size 512 × 512 by our algorithm. The experiment results show that the presented algorithm can efficiently re- colorize the color images with reserving the contours of original images and has advantage that using the best fitting function to determine the pixel value of each pixel to re- colorize the color image is time saving largely. With this algorithm, one can successfully and effectively re- colorize the color image no matter it is of uniform color or complex colors so it is suitable to be used in the design of virtual reality and the recognition of color image.

REFERENCES

[1] R. Kawakami, K. Ikeuchi, R.T.Tan, Consistent Surface Color for Texturing Large Objects in Outdoor Scenes, *Tenth IEEE International Conference on Computer Vision*, 2(2005) 1200 – 1207

[2] Bosch , X. Mun˜oz, J. Freixenet,Segmentation and description of natural outdoor scenes,

I*mage and Vision Computing* 25 (2007) 727–740

[3] J. Batlle, A. Casal, J. Freixenet, J. Mart, A review on strategies for recognizing natural objects in colour images of outdoor scenes, *Image and Vision Computing* 18 (2000) 515–530

[4] Van de Hulst HC, Light Scattering by small particles, *Dover Publications*, New York, 1981.

[5] M. Sneep, W. Ubachs, Direct measurement of the Rayleigh scattering cross section in various gases, *Journal of Quantitative Spectroscopy & Radiative Transfer*. 92 (2005) 293- 310.

[6] R. V. Deelen, J. Landgraf, I. Aben, Multiple elastic light scattering in the Earth's atmosphere: a doubling-adding method to include rotational Raman scattering by air, *Journal of Quantitative Spectroscopy & Radiative Transfer*. 95 (2005) 309- 330.

[7] S. M. Lea, J. R. Burke, Physics: The nature of things, annotated instructor's edition 1997, *West Company*, USA, 597-626.

[8] W. B. Thompson, P. Shirley, J. A. Ferwer, A Spatial Post- Processing Algorithm for Images of Night Scenes, *Journal of Graphics Tools*. 7 (1), (2003) 1- 12.

[9] T. Welsh, M. Ashikhmin, K. Mueller, Transferring color to grayscale images. Proceedings of 29th annual conference on computer graphics and interactive techniques, *ACM Press*, New York, USA, 2002, pp. 277–280.

[10] Toet, Colorizing single band intensified night vision images, *Displays*.26 (1), (2005) 15-21.

[11] M. Brown, A step-by-step guide to non-linear regression analysis of experimental data using a Microsoft Excel spread sheet, *Computer methods and programs in Biomedicine*. 65 (2001) 191-200.

[12] J. Vianna, E. A. De Souza, Combining Marr and Canny Operators to Detect Edges, *Microwave and Optoelectronics Conference*. 2 (2003) 695-699.

[13] G. W. Larson, H. Rushmeier, C. Piatko, A Visibility Matching Tone Reproduction Operator for High Dynamic Range Scenes, *IEEE Trans. On Visualization and Computer Graphics*. 3 (4), (1997) 291-236.

[14] J. A. Ferwerda, Elements of Early Vision for Computer Graphics, *IEEE Computer Graphics and Applications*. 21 (5), (2001) 22-33.

[15] M. Boutell, J. Luo, Sunset Scene Classification Using Simulated Image Recomposition, Proceeding, *IEEE Int'l Conf. on Multimedia and Expo.* (2003) I.37-I.40.

[16] Vapnik VN, The nature of statistical learning theory, *New York: Springer*, 1995.

[17] K. Y. Chen, Forecasting systems reliability based on support vector regression with genetic algorithms, *Reliability Engineering and System Safety*. 92 (2007) 423-432.

[18] Clausen, H. Wechsler, Color Image Compression Using PCA and Backpropagation Learning, *pattern recognition*. 33 (2000)1555-1560.

[19] T. Bose, Digital signal and image processing, J. Wiley & sons, New York, 2004. Andreadis, Ph. Tsalides, Analog computation of Image Chromaticity, *Real-Time Imaging* 3 (1997)1-6.

[20] N. Božinović, J. Konrad, Motion analysis in 3D DCT domain and its application to video coding, *Signal Processing: Image Communication*.20 (2005) 510-528.

[21] D.J. Duh, J.H. Jeng, S.Y. Chen, DCT based simple classification scheme for fractal image compression, *Image and Vision Computing*. 23 (13) (2005) 1115-1121.

[22] S. Liu, A. C. Bovik, Foveation embedded DCT domain video transcoding, *Journal of Visual Communication and Image Representation.* 16 (6) (2005) 643-667.